

Modelling Tidal Energy Extraction in a Depth-Averaged Coastal Domain

S. Draper¹, G.T. Houlsby, M.L.G. Oldfield and A.G.L. Borthwick

¹ Department of Engineering Science,
University of Oxford,
Parks Road, Oxford, OX1 3PJ, UK
E-mail: scott.draper@eng.ox.ac.uk

Abstract

Numerical models have been used recently to quantify the effects of tidal extraction in specific tidal systems. Commonly, these studies have employed numerical approximations to the depth-averaged shallow water equations to simulate tidal hydrodynamics. Tidal power extraction has then been introduced by incorporating an additional bed shear source term, or another general source term, to represent the presence of tidal devices.

We review these models and adopt an approach, based on actuator disc theory, to define the properties of a tidal device within a depth-averaged numerical model. This approach allows a direct link to be made between the actual tidal device and the equivalent momentum sink that the device should impart within a two dimensional (2D) depth-averaged domain. We use this description of a tidal device to model the hydrodynamic effects of energy extraction in an arbitrary coastal domain.

Keywords: actuator disc, resource assessment, shallow water equations, tidal power.

Nomenclature

A	=	Area of a turbine(s)
a	=	Amplitude of a tidal constituent
B	=	Blockage ratio
b	=	Uniform channel width
C	=	Dimensionless coefficient
$F(\)$	=	Numerical flux
Fr	=	Froude number
f	=	Coriolis parameter
g	=	Acceleration due to gravity
h	=	Depth of water
Δh	=	Change in depth
k	=	Dimensionless drag coefficient
P	=	Power
Q	=	Flow rate

T	=	Thrust exerted from a turbine(s) to the fluid
u, v	=	Depth averaged velocity components
X	=	Net force between turbine and bypass flows
x, y	=	Cartesian co-ordinate system
α, β	=	Velocity coefficients
γ	=	Multiplier
η	=	Efficiency
ρ	=	Fluid density
τ	=	Shear stress
ζ	=	Wave height

Subscripts

$1, 2, \dots$	=	Stations
b	=	Bypass streamtube
d	=	Dimensionless drag
h, v	=	Horizontal and vertical directions
max	=	Maximum value
m	=	Boundary value internal to a finite volume
n	=	Normal component to a turbine fence
P	=	Dimensionless power
p	=	Boundary value external to a finite volume
s	=	Still water level
T	=	Dimensionless thrust
t	=	Turbine streamtube
W	=	Wake
x, y	=	Cartesian components
*	=	Maximum average value
+	=	Outside finite volume boundary
-	=	Inside finite volume boundary

Superscripts

*	=	Solution at flux interface
---	---	----------------------------

1 Introduction

The deployment of a large scale tidal farm will influence the hydrodynamics within a coastal basin. Given the associated environmental and commercial costs that might be associated with this influence, there is need for better understanding of the hydrodynamic impacts of large scale energy extraction.

Although analytical theoretical models exist, it is expected that further understanding will be provided by means of numerical simulations which model depth-averaged hydrodynamics. For these numerical simulations to provide realistic insight, the models employed must be accurate and must allow for a realistic definition of energy extraction within the coastal basin.

The layout of this paper is as follows. We begin by reviewing the literature on theoretical and numerical modelling of tidal power extraction in coastal systems. Next, in an effort to define energy extraction in a numerical model, we discuss the actuator disc model for tidal turbines due to Whelan *et al.* [1], and provide some additional discussion on downstream mixing and head efficiency. We argue, using simple scaling assumptions, that actuator disc theory can provide a useful definition for tidal power extraction in coastal basins. Lastly we discuss the extraction of power from a channel and compare the results with an analytical model due to Garrett and Cummins [2].

2 Literature Review

One Dimensional Theoretical Models

Two one dimensional (1D) theoretical models have been developed to describe energy extraction from a channel. The first, due to Garrett and Cummins [2], investigates a channel connecting two large bodies of water which differ in tidal phase and/or amplitude. For instance, this could be a strait between an island and a large land mass, or simply a strait between two otherwise disconnected oceans. A similar theoretical model, due to Garrett and Cummins [3] and Blanchfield *et al.* [4], concerns a channel connecting a large basin/ocean to an enclosed basin/bay. It is a generalised form of the first model discussed above, if the two large basins are only connected through the channel [4].

Together these two models cover many realistic coastal systems in which tidal energy extraction might be attractive, and might, for instance, represent a first approximation for the Pentland Firth. Other sites, such as flow around a headland [5, 17], are not covered by the theories. However, given the generality of the 1D models it is useful to discuss their implications.

Both of the 1D theories adopt the 1D dynamic equation to describe flow through the channel, and make several simplifying assumptions discussed in [2, 4, 6]. Based on these assumptions a maximum average power that can be extracted from the channels, when subjected to a sinusoidal driving tide of amplitude a , is shown to be [2, 4]:

$$P_* = \gamma \rho g a Q_{\max} \quad (1)$$

where Q_{\max} is the maximum flow rate in the undisturbed channel and the dimensionless factor γ ranges between 0.21 and 0.24 for the first theory and between 0.19 and 0.26 for the second. This range in γ is representative of the dynamic balance in the channel, with a value of 0.21 in both models indicating that the flow is dominated by natural drag as opposed to acceleration effects [2, 4]. However, since the range in γ is small, taking $\gamma=0.22$ provides a useful approximation to both regimes [2, 4]. Furthermore, using this value the maximum average power is defined in terms of only the undisturbed flow rate and the driving amplitude, both of which are measureable from observations and numerical models, and therefore the analysis requires no detailed understanding of the dynamical balance in the channel [2, 6, 7]. Determining if exit separation or other non-linear losses are important in the dynamic balance becomes unnecessary provided that these terms vary, to the leading order, with the flow rate squared as turbines are introduced [6, 8].

In addition to predicting the maximum power, the models also provide an indication of hydrodynamic effects. At maximum average power extraction the flow rate for a channel between two large basins is reduced to 58% if drag forces are dominant in the undisturbed state [2] (this value has also been given by Bryden and Couch [11]). This reduction might be unacceptable environmentally. However, if only a 10% reduction in the flow rate is acceptable, then it is easy to show that 44% of maximum average power can still be achieved (when $\gamma=0.21$) [7]. For the second theory, a similar trend is noted as reduced power is extracted [8, 12].

As discussed in the next subsection, both theories have been compared, with reasonable agreement, to 2D numerical simulations for uniform extraction across a real channel. Garrett and Cummins [9] have suggested one way to extend the theory to account for a channel that is partially blocked with the use of linear momentum actuator disc theory (LMADT) applied in the region of the turbines. However, although actuator disc theory ties in well with the assumptions of the 1D theoretical models, it also requires further assumptions in the vicinity of the power extraction, such as the requirement for a constant channel width, a uniform along channel bathymetry, uniform upstream flow and steady state conditions. Furthermore, no account can be made for asymmetry in the placement of a partial turbine fence.

In summary, the 1D theoretical models provide a reasonably complete explanation of the physics of tidal energy extraction from coastal channels. Numerical simulations, or alternative theoretical models, will provide additional insight for fully two dimensional systems, such as flow around a headland [17], and for channels with highly non-uniform geometry and asymmetrically placed turbine fences that partially block the channel.

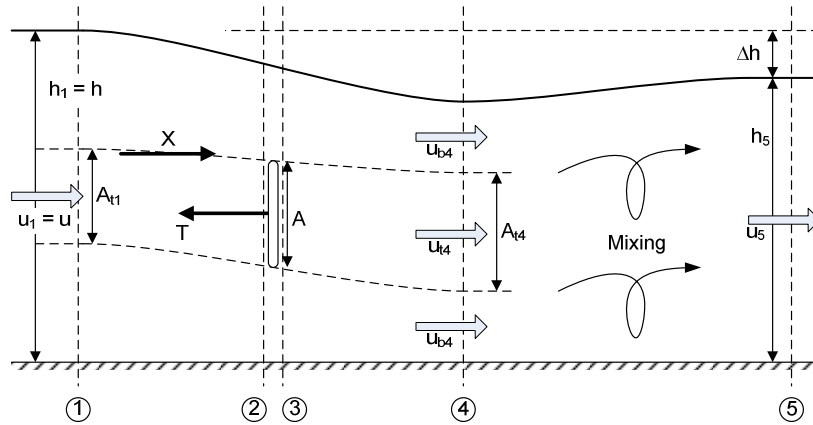


Figure 1: One dimensional linear momentum actuator disc theory in an open channel flow [16].

2D Numerical Simulations

Several site-specific numerical simulations have been documented. Amongst these are a study of the Johnstone Strait by Sutherland *et al.* [7], of the Minas Passage by Karsten *et al.* [8] and of the Portland Bill by Blunden and Bahaj [5, 10].

The first two of these studies make direct comparison with the 1D theoretical models discussed above. For example, the study of the Minas Passage, which connects the Bay of Fundy and the open ocean to the Minas Basin, is similar to the second theoretical model above [8]. The maximum average power calculated by the numerical model is found to be 87% of that predicted by Eq. 1, where the amplitude used in Eq. 1 is the amplitude of the forcing tides [8].

The study of the Johnstone Strait considers several scenarios, the first two of which match reasonably well with the first theoretical model discussed above [7]. For these scenarios, applying a uniform extraction of energy across the Strait provided a numerical maximum average power that agreed with Eq. 1 to within 10% [7]. This result is similar when the amplitude in Eq. 1 is taken to be that at the inlet to the Strait, both without and with energy extraction.

The third site-specific analysis conducted in [5, 10] is not covered by the theories discussed above, since it considers a two dimensional flow around a headland [5]. However, simulations without extraction are compared to observations, and a mesh convergence study is conducted. The spatial effects of extracting a given amount of power are reported, with contour plots that display co-tidal lines and tidal ellipse parameters both with and without power extraction.

In all of the site-specific studies, the installation of tidal turbines is accounted for in the numerical model by the addition of a bed friction source term which varies with the square of the local tidal current velocity. For example, in both [7] and [8] the friction coefficient is defined as:

$$C_d = k_o + k_t, \quad (2)$$

where k_o is related to natural friction and k_t represents tidal turbines. Since the objective of [7] and [8] was to investigate the maximum extractible power, no particular physical description of k_t is discussed. However, in [5, 10] the coefficient was assigned based on a case study of a yawed horizontal axis marine current turbine and a hypothetical array design.

Discussions of tidal device farms that are not uniform across a tidal channel are also made by [7] and [8], and implicitly by [5]. For instance, Karsten *et al.* [8] simulate the effects of introducing bed roughness over only part of the Minas Passage, and show that the efficiency of the tidal extraction is reduced. Whilst Sutherland *et al.* [7] mention that preliminary studies have shown that extraction is ineffective for turbines that occupy only a part of the channel. All three studies suggest that the local effects of turbines, which occupy only a fraction of the flow, could be introduced into a depth averaged model by means of a three dimensional, or fully discretized, local model [5, 7, 8].

In addition to the site specific studies, general coastal basins have also been studied by Bryden and Couch [13] and Polagye *et al.* [14]. In the first of these, flow around an island is considered. The velocity and depth profiles at several cross sections are estimated, both with and without energy extraction, and the turbines are introduced by an added roughness. In [14], the 1D shallow water equations are solved in a uniform channel which has one open boundary, one closed boundary and two discontinuous changes in width that define an internal extraction zone. Based on the argument that vertical mixing in the wake of the turbine has a length scale that is much smaller than the mesh size, extraction effects from tidal turbines are introduced as line discontinuities across the complete width of the extraction zone. Changes to estuary geometry, tidal regime and non-linear turbine dynamics are then investigated, with results showing that reductions in flow volume and power density, in addition to spatial variation in tidal range and tidal phase, occur as a result of energy extraction.

3 Momentum Actuator Disc Theory

The LMADT presented in [9] considers an actuator disc in a flow of constant cross section, bounded by parallel channel walls and a constant depth free surface. Recently, an application of LMADT for finite Froude number has been developed by Whelan *et al.* [1] to provide an approximation to the flow field around an actuator disc in an open channel flow with a non constant free surface [1, 15].

One advantage of this second theory is that, after introducing downstream mixing, it provides a local steady state description of a real turbine, or line of turbines, that can be introduced as a perturbation in both velocity and depth into a depth averaged numerical model. Figure 1 illustrates a one dimensional channel with an actuator disc. This figure depicts the theory described in [1], but includes downstream mixing. As in [1], it is assumed that there is a uniform upstream velocity u , depth h and constant width b , and that the flow is inviscid.

The flow in Figure 1 is analysed at various stations. At Stations 1, 4 and 5 it is assumed that the pressure is hydrostatic and the flow is uniform. The velocity $u_{b4} = \beta_4 u$ denotes the bypass flow velocity at Station 4, while $u_{t2} = \alpha_2 u$ and $u_{t4} = \alpha_4 u$ define the turbine flow velocity at Stations 2 and 4 respectively. The thrust T is the horizontal force applied to the fluid from the turbine, and the force X implies a constraining force between the turbine streamtube and the bypass flow. Finally the turbine has an area A , such that a dimensionless blockage ratio may be defined as $B = A/(hb)$.

Following [1], applying continuity, energy and momentum conservation selectively between Stations 1 and 4 leads to a quartic equation describing the bypass velocity:

$$\frac{Fr^2}{2}\beta_4^4 + 2\alpha_4 Fr^2 \beta_4^3 - (2 - 2B + Fr^2)\beta_4^2 - (4\alpha_4 + 2\alpha_4 Fr^2 - 4)\beta_4 + \left(\frac{Fr^2}{2} + 4\alpha_4 - 2B\alpha_4^2 - 2\right) = 0, \quad (3)$$

where $Fr = u/\sqrt{gh}$ is the upstream Froude number. The solution of this equation for β_4 allows the calculation of all the other velocity coefficients. The power and thrust can then be determined in terms of a power coefficient C_P and a thrust coefficient C_T :

$$T = \frac{1}{2}\rho u^2 Bbh(\beta_4^2 - \alpha_4^2) = C_T \frac{1}{2}\rho u^2 Bbh, \quad (4a)$$

$$P = \alpha_2 u T = \frac{1}{2}\rho u^3 Bbh\alpha_2(\beta_4^2 - \alpha_4^2) = C_P \frac{1}{2}\rho u^3 Bbh. \quad (4b)$$

Since the flow is not uniform with depth at Station 4, we assume that downstream mixing will occur.

Applying momentum conservation in the horizontal direction between Stations 1 to 5 then leads to:

$$\frac{1}{2}\rho g b(h^2 - (h - \Delta h)^2) - T = \rho b h u \left(\frac{uh}{h - \Delta h} - u \right).$$

Substituting for the thrust coefficient and rearranging then gives:

$$\frac{1}{2}\left(\frac{\Delta h}{h}\right)^3 - \frac{3}{2}\left(\frac{\Delta h}{h}\right)^2 + \left(1 - Fr^2 + \frac{C_T B Fr^2}{2}\right)\frac{\Delta h}{h} - \frac{C_T B Fr^2}{2} = 0. \quad (5)$$

This is a cubic that can be solved for the downstream depth change $\Delta h = h - h_5$. We can also determine the power lost in the wake in terms of this depth change:

$$P_W = \frac{1}{2}\rho u^3 Bbh\alpha_2\alpha_4^2 + \frac{1}{2}\rho u^3 bh(1 - B\alpha_2) - \frac{1}{2}\rho u^3 bh\left(\frac{h}{h - \Delta h}\right)^2 + hbu(h_4 - h_5)\rho g \quad (6)$$

Combining Eq. 6 with Eq. 4b then gives the total power lost in the channel:

$$P + P_W = \rho g ubh\Delta h \left(1 - Fr^2 \frac{1 - \Delta h/2h}{(1 - \Delta h/h)^2} \right), \quad (7)$$

and a measure of head efficiency follows directly:

$$\eta = \frac{P}{P + P_W} = \frac{P}{\rho g ubh\Delta h \left(1 - Fr^2 \frac{1 - \Delta h/2h}{(1 - \Delta h/h)^2} \right)^{-1}}. \quad (8)$$

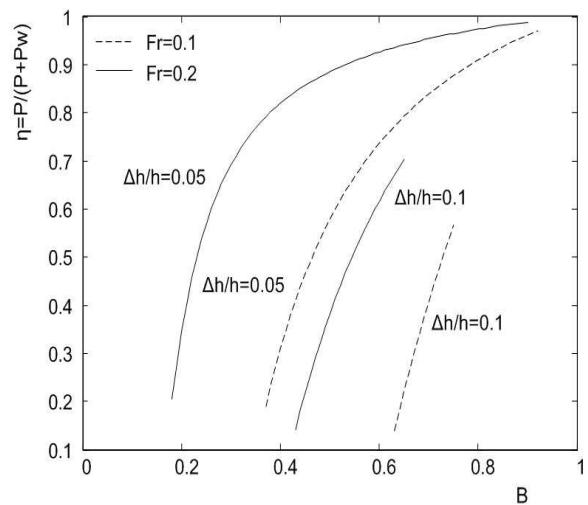


Figure 2: Efficiency as a function of blockage ratio. The curves are truncated for high blockage ratio when supercritical flow results, and for low blockage ratio when the extraction of the specified power becomes impossible.

We can make several observations about this measure of efficiency and its design implications for tidal turbines.

Firstly, as the Froude number becomes small, Eq. 8 agrees with the analysis of Garrett and Cummins [9] for an actuator disc in a constrained volume flow:

$$\eta = \frac{P}{P_{REF}} = \frac{P}{u A_C \Delta p},$$

where $A_C = bh$, $P_{REF} = P + P_W$ and Δp is interpreted as $\rho g \Delta h$.

Secondly, both the measure of efficiency defined by Garrett and Cummins above, and that for finite number Froude (Eq. 8), are optimized when the downstream flow limits to that of the upstream flow, or rather no power is removed. However, a more interesting problem arises if we fix the available reference power or equivalently constrain the downstream depth change (possibly for environmental reasons), and optimize efficiency subject to this constraint.

For a given Froude number and downstream depth change, we then find that the efficiency increases with increasing blockage ratio. Figure 2 shows the efficiency as a function of blockage ratio for a fixed downstream allowable depth change of 5% and 10%.

As an alternative to increasing the blockage ratio, efficiency can also be improved by increasing the number of turbines, placed in series, to extract the overall constrained downstream head change. Figure 3 shows the net efficiency for a channel of numerous turbines, each extracting an equal proportion of the total downstream depth change and positioned in series so that complete mixing occurs between successive turbines.

The measure of efficiency given by Eq. 8 therefore implies some interesting design rules for tidal turbines in the presence of environmental constraints.

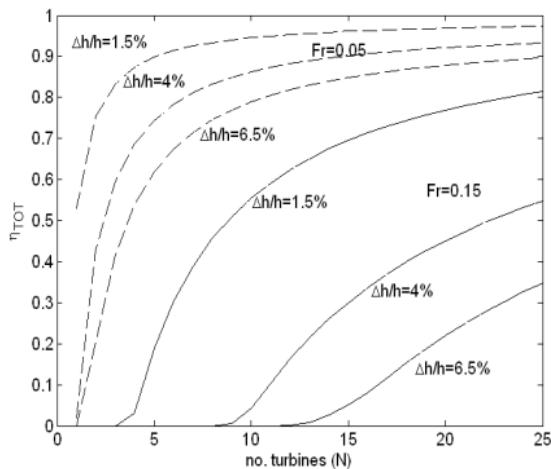


Figure 3: Efficiency as a function of the number of turbines used in series to extract energy. The total downstream depth change is labeled. $Fr=0.05$ (dashed lines), $Fr=0.15$ (solid line).

4 Use of Actuator Disc Theory in a Depth-Averaged Dynamic Model

We now discuss how a row of turbines might be defined in a 2D depth-averaged numerical model using LMADT. For example, two typical scenarios for a row of turbines are illustrated in Figure 4. The first is a fence that extends completely across a channel. In this case the perturbation to the free surface at each discrete location across the fence is given directly by Eq. 5, provided that the flow through the fence is quasi-steady. If the mixing length of the turbine wake is small compared to the tidal wavelength, this last assumption should be satisfied. The numerical implementation for this scenario is discussed in Section 5.

The second scenario, in Figure 4b, considers a fence that only partially blocks an irregular channel. In this case the channel might be too irregular for an assumption of uniform flow, the turbines might be asymmetrically located, or the total mixing length due to the turbines may be long relative to the tidal wavelength. However, despite this we may still employ LMADT on the basis of some scaling assumptions. For instance, we define two mixing lengths, as shown in Figure 4b. The first of these is a vertical mixing length l_v , after which vertical variations in wake velocity become negligible. The second is a lateral mixing length l_h , after which horizontal variations in the total across channel wake velocity become negligible. If the channel is irregular over the distance l_h then the use of LMADT to define mixing over this length is invalid. However, if we assume that $l_v \ll l_h$, and that both mixing process are somewhat independent, it is reasonable to assume that LMADT could be used to provide a perturbation to the flow over the vertical mixing length l_v . This amounts to using only a vertical blockage ratio for the turbines. The numerical model then simulates the lateral mixing process.

Further investigation is being undertaken to validate this approach.

5 Numerical Modelling

Two-dimensional depth averaged shallow flow models are commonly adopted to model tidal hydrodynamics in coastal basins:

$$\frac{\partial h}{\partial t} + \frac{\partial(uh)}{\partial x} + \frac{\partial(vh)}{\partial y} = 0, \quad (9a)$$

$$\frac{\partial(uh)}{\partial t} + \frac{\partial(u^2h)}{\partial x} + \frac{\partial(uvh)}{\partial y} = -gh \frac{\partial \zeta}{\partial x} - \frac{\tau_x}{\rho} + fvh, \quad (9b)$$

and,

$$\frac{\partial(vh)}{\partial t} + \frac{\partial(uvh)}{\partial x} + \frac{\partial(v^2h)}{\partial y} = -gh \frac{\partial \zeta}{\partial y} - \frac{\tau_y}{\rho} - fuh, \quad (9c)$$

where $h = h_s + \zeta$ is the total water depth and h_s is the still water depth, u and v are the horizontal depth averaged velocity components aligned with the x and y axis respectively, f is the Coriolis parameter and, τ_x and τ_y are frictional stress terms due to bed friction.

Several extensions can be made to this set of equations to account for more complex physics. These may include, for example, Boussinesq terms for dispersion, and depth averaged viscosity for turbulent diffusion. In this work we solve this set of equations with the discontinuous Galerkin finite element method [18, 19].

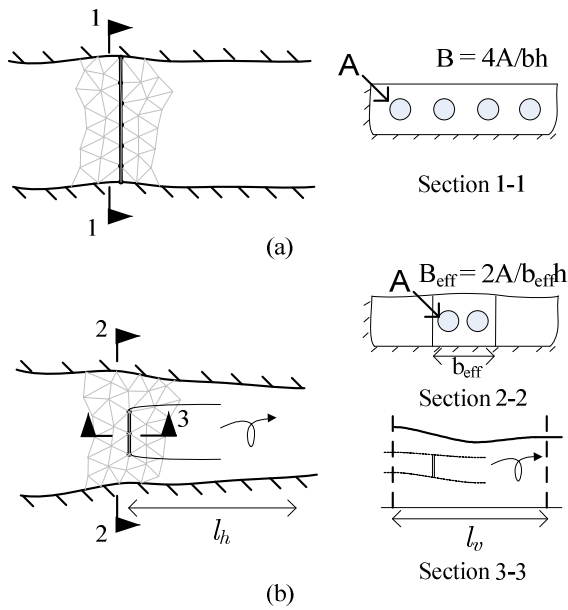


Figure 4: Two channels containing a fence of tidal turbines.

5.1 Introducing Tidal Turbines

In a depth averaged model there are two basic options for introducing a steady state local solution, such as that provided by LMADT, to describe a fence of tidal turbines (see Figure 4a). The best choice typically depends on the spatial discretization of the numerical model. For example, if the length scale of the turbine wake (or vertical wake for a partial fence) is much smaller than the mesh size, introducing turbines in the form of a line discontinuity becomes physically realistic [14]. However, if the mesh size is of the order of the turbine wake length, then the introduction of an additional bed roughness, spatially averaged or otherwise, into the governing equations might be a suitable approach. We now briefly summarise the first of these approaches for a finite volume type scheme.

The introduction of a line of turbines into any finite volume scheme (or the discontinuous Galerkin method) as a line discontinuity can be achieved by a modification to the numerical flux. For instance,

consider Figure 5, which displays the interface between two finite volumes aligned with a fence of tidal turbines. The outward pointing normal to the left finite volume is in the direction x_n . To determine the appropriate numerical flux we first interpolate the values h_m, \bar{u}_m, h_p and \bar{u}_p (where the overbar indicates the component in the coordinate direction x_n) either side of the interface directly from the discrete solution. These values are then used, together with a definition of the turbine and knowledge of the characteristic invariants, to determine the flux out of the left finite volume $F(h_-^*, \bar{u}_-^*)$ and the flux into the right finite volume $F(h_+^*, \bar{u}_+^*)$. The four equations defining $h_-^*, \bar{u}_-^*, h_+^*$ and \bar{u}_+^* are:

$$\bar{u}_m + 2\sqrt{gh_m} = \bar{u}_-^* + 2\sqrt{gh_-^*}, \quad (10a)$$

$$\bar{u}_p - 2\sqrt{gh_p} = \bar{u}_+^* - 2\sqrt{gh_+^*}, \quad (10b)$$

$$h_- \bar{u}_-^* = h_+ \bar{u}_+^*, \quad (10c)$$

and,

$$\Delta h^* = h_-^* - h_+^* = G(h_\pm^*, u_\pm^*), \quad (10d)$$

where G is any arbitrary function that defines the properties of the tidal turbines. As an example, Polagye *et al.* [14] have used an energy compatibility relationship for Eq. 10d for a 1D channel.

Another obvious choice is to adopt the LMADT discussed in Section 3. Using this relationship the function G is given by Eq. 5, noting that C_T and Fr are functions of the upstream depth h_{up} and velocity u_{up} chosen appropriately from h_m, \bar{u}_m, h_p and \bar{u}_p .

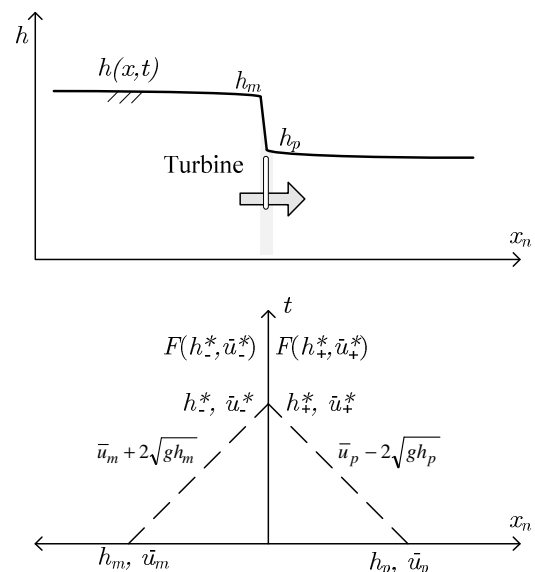


Figure 5: Discontinuous solution and characteristic conditions at an interface between two finite volumes aligned with a tidal turbine fence.

6 A Simple Channel

In this last section we consider a simple straight channel between two large basins. The purpose of the simulation is to test the method of introducing turbines into the Discontinuous Galerkin method, as discussed in Section 5, and to compare the numerical solution with that obtained from the first theoretical model, due to Garrett and Cummins [2], discussed in Section 2.

We consider two channels with geometry (and mesh) defined in Figure 6 and Table 1. In both channels the initial water depth is set constant at 70 m. The curved open boundary of the left basin is then forced with a sinusoidal tide of amplitude 1.0 m and an angular frequency 0.00014 rad/s until maximum amplitude is reached after 3.1 hrs. The depth at this left open boundary is then held constant. The depth variation on the curved open boundary of the right basin is kept at zero throughout. After 48 hrs the flow within the channel was deemed to have reached steady state conditions, allowing for a numerical comparison to the quasi-steady analytical model discussed in Section 2.

	L [km]	B [km]	R [km]	Q_{\max} [$\times 10^6 \text{m}^3/\text{s}$]	P_{\max} [MW]
Channel 1	30	4	4	0.819	3090
Channel 2	10	4	4	1.34	5075

Table 1: Geometry of channels. The bottom friction for both channels was set at $C_d = 0.003$.

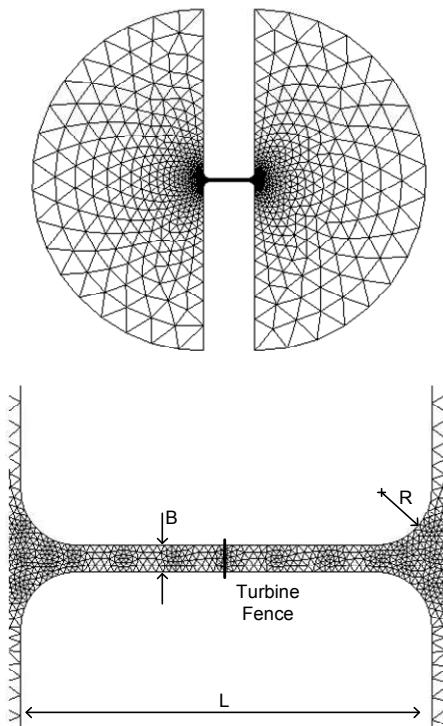


Figure 6: Numerical mesh for the simple channel (Channel 1 mesh shown). For both channels the semi-circular basins have a radius of 100 km.

Initially, for a case with no turbine fences, the flow rates in both of the channels were obtained and recorded as Q_{\max} in Table 1. The predicted maximum power, given in [2] as $P_{\max} = 0.38\rho g a Q_{\max}$, was then evaluated for both channels (Table 1). To investigate whether the numerical model is in agreement a fence of turbines located across the middle of the channel is introduced (see Figure 6). The discontinuity across the fence is defined using LMADT, as explained in Section 5, for a real fence of turbines operating at approximately maximum power output ($\alpha_4 = 1/3$). The power extracted by the fence P , and the flow rate in the channel Q , are computed for a range of turbine blockage ratios. Figure 7 compares these simulated power and flow rates, normalised by their predicted and measured maximum values respectively, to the predicted theoretical results. The agreement between theory and the numerical simulations is good. In general this indicates that both friction and separation losses do decrease with the flow rate squared for both channels when turbines are added. For the short channel in particular, where separation losses are more important, this also implies that the point at which the flow exits the channel as a jet is relatively constant despite the addition of turbines.

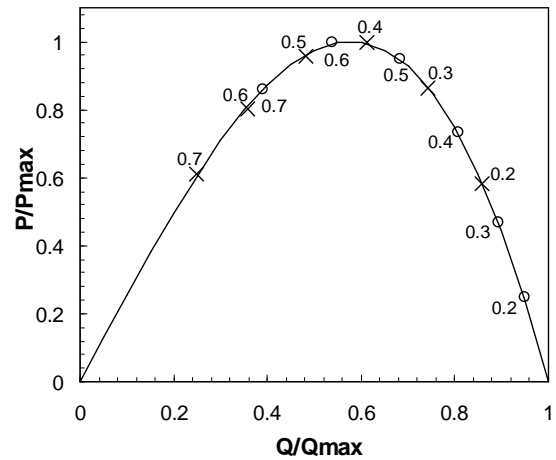


Figure 7: Numerical power (normalised by predicted maximum power) plotted against flow rate (normalised by the undisturbed flow rate) for Channel 1 (o's), Channel 2 (x's), and the theoretical prediction due to [2] (line). The numbers correspond to blockage ratio.

In Figure 7 it is also clear that a lower blockage ratio is required to reach maximum power for the short channel ($B=0.4-0.5$), where friction drag is a higher proportion of total losses, than the long channel ($B=0.5-0.6$). This result is predicted by the theory and discussion in [6] where, for a small Froude number, the optimal blockage ratio is noted to be an increasing function of friction losses. In the case of only separation losses, and therefore no friction losses, the optimal blockage ratio is given as

approximately 0.46 when the channel area at the location of the turbines is equal to the channel area at the exit [6]. For both channels in Table 1 we note that the exit area is greater than the channel area at the turbines, and so this lower bound reduces slightly (for example the lower bound would be approximately 0.39 if the exit area is 25% larger), which is consistent with the results in Figure 7.

In summary the simulations provide a cross-validation between the theory and the analysis for this simple geometry. This gives confidence in applying the numerical technique to more complex systems that cannot be addressed by the simple theory.

7 Conclusions

Two existing 1D theoretical models provide a good understanding of the effects of energy extraction from tidal turbines in channels. However, further work with numerical simulations is required to test the limitations of these theories, such as for partially blocked irregular channels, and to provide a general understanding for truly 2D tidal systems.

LMADT provides an efficiency measure for a tidal turbine in an open channel flow with free surface effects. This measure indicates that increasing the blockage ratio of tidal turbines, and increasing the number of turbines placed in series downstream, will improve efficiency.

Furthermore, LMADT is a convenient theory that can be used to introduce a line, or fence, of tidal turbines into a depth averaged numerical model.

Acknowledgements

The first author acknowledges the support of the Rhodes Trust.

References

- [1] J.I. Whelan, J.M. Graham and J. Peiro. A free-surface and blockage correction for tidal turbines. *Journal of Fluid Mechanics*. 624:281-291, 2009.
- [2] C. Garrett and P. Cummins. The power potential of tidal currents in channels. *Proc. R. Soc. Lond. A* 461:2563-2572, 2005.
- [3] C. Garrett and P. Cummins. Generating Power from Tidal Currents. *J. Waterway, Port, Coastal and Ocean Engineering*. 130:114-118, 2004.
- [4] J. Blanchfield, C. Garrett, P. Wild and A. Rowe. The extractable power from a channel linking a bay to the open ocean. *Proc. IMechE Part A: J. Power and Energy*. 222:289-297, 2008.
- [5] L.S. Blunden and A.S. Bahaj. Effects of tidal energy extraction at Portland Bill, southern UK predicted from a numerical model. *Proc. 7th EWTEC*, Porto, Portugal, 2007.
- [6] C. Garrett and P. Cummins. Limits to tidal current power. *Renewable Energy* 33:2485-2490, 2008.
- [7] G. Sutherland, M. Foreman and C. Garrett. Tidal current energy assessment for Johnstone Strait, Vancouver Island. *Proc. IMechE Part A: J. Power and Energy*. 221:147-157, 2007.
- [8] R.H. Karsten, J.M. McMillan, M.J. Lickley and R.D. Haynes. Assessment of tidal current energy in the Minas Passage, Bay of Fundy. *Proc. IMechE Part A: J. Power and Energy*. 222:493-507, 2008.
- [9] C. Garrett and P. Cummins. The efficiency of a turbine in a tidal channel. *Journal of Fluid Mechanics*. 588:243-251, 2007.
- [10] L.S. Blunden and A.S. Bahaj. Initial evaluation of tidal stream energy resources at Portland Bill, UK. *Renewable Energy*. 31:121-132, 2006.
- [11] I. G. Bryden and S.G. Couch. How much energy can be extracted from moving water with a free surface: A question of importance in the field of tidal current energy. *Renewable Energy*. 32:1961-1966.
- [12] J. Blanchfield, C. Garrett, P. Wild and A. Rowe. Tidal stream power resource assessment for Masset Sound, Haida Gwaii. *Proc. IMechE Part A: J. Power and Energy*. 222:485-492, 2008.
- [13] I. G. Bryden, S. J. Couch, A. Owen and G. Melville. Tidal current resource assessment. *Proc. IMechE Part A: J. Power and Energy*. 221:125-135, 2007.
- [14] B. Polagye, P. Malte, M. Kawase and D. Durran. Effect of large-scale kinetic power extraction on time-dependent estuaries. *Proc. IMechE Part A: J. Power and Energy*. 222:471-484, 2008.
- [15] J. I. Whelan, M. Thomson, J.M.R. Graham and J. Peiro. Modelling of free surface proximity and wave induced velocities around a horizontal axis tidal stream turbine. *Proc. 7th EWTEC*, Porto, Portugal, 2007.
- [16] G.T. Housby, S. Draper and M. Oldfield. Application of Linear Momentum Actuator Disc Theory to Open Channel Flow. Technical Report 2296-08, OUEL, 2008.
- [17] L. S. Blunden and A. S. Bahaj. Tidal energy resource assessment for tidal stream generators. *Proc. IMechE Part A: J. Power and Energy*. 221:137-146, 2007.
- [18] C. Eskilsson and S.J. Sherwin. A triangular spectral/hp discontinuous Galerkin method for modelling the 2D shallow water equations. *International Journal for Numerical Methods*. 45:605-623, 2004.
- [19] F. X. Giraldo and T. Warburton. A high-order triangular discontinuous Galerkin oceanic shallow water model. *International Journal for Numerical Methods*. 56:899-925, 200.